CHIN. PHYS. LETT. Vol. 34, No. 10 (2017) 107401

High-Quality $FeTe_{1-x}Se_x$ Monolayer Films on $SrTiO_3$(001) Substrates Grown by Molecular Beam Epitaxy *

Zhi-Qing Han(韩智卿)[1], Xun Shi(施训)[2], Xi-Liang Peng(彭锡亮)[2],
Yu-Jie Sun(孙煜杰)[2**], Shan-Cai Wang(王善才)[1**]

[1]*Department of Physics, Beijing Key Laboratory of Opto-Electronic Functional Materials and Micro-nano Devices, Renmin University of China, Beijing 100872*
[2]*Beijing National Laboratory for Condensed Matter Physics, and Institute of Physics, Chinese Academy of Sciences, Beijing 100190*

(Received 19 June 2017)

We report the growth process of $FeTe_{1-x}Se_x$ ($0 \le x \le 1$) monolayer films on $SrTiO_3$ (STO) substrates through molecular beam epitaxy and discuss the possible ways to improve the film quality. By exploring the parameters of substrate treatment, growth control and post growth annealing, we successfully obtain a series of $FeTe_{1-x}Se_x$ monolayer films. In the whole growth process, we find the significance of the temperature control through surface roughness monitored by the reflection high-energy electron diffraction and scanning tunneling microscopy. We obtain the best quality of FeSe monolayer films with the STO substrate treated at $T = 900$–$950°C$ before growth, the FeSe deposited at $T = 310°C$ during growth and annealed at $T = 380°C$ after growth. For $FeTe_{1-x}Se_x$ ($x < 1$), both the growth temperature and annealing temperature decrease to $T = 260°C$. According to the angle-resolved photoemission spectroscopy measurements, the superconductivity of the $FeTe_{1-x}Se_x$ film is robust and insensitive to Se concentration. All the above are instructive for further investigations of the superconductivity in $FeTe_{1-x}Se_x$ films.

PACS: 74.70.Xa, 61.05.jh, 68.37.Ef DOI: 10.1088/0256-307X/34/10/107401

Among the iron-based superconductors, the $FeTe_{1-x}Se_x$ system is of particular interest.[1–4] It has the simplest PbO structure ($P4/nmm$)[5,6] with its internal parameters systematically tuned by the substitution of Te by Se,[7–9] which is helpful to study superconducting mechanisms. The superconductivity in $FeTe_{1-x}Se_x$ has been observed in a wide range of compositions,[2–4] with its maximum superconducting transition temperature $T_c \approx 14.5$ K and superconducting gap $\Delta \approx 1.7$ meV at $x = 0.4$.[2–4,10–23] The superconducting transition temperature can be further enhanced by pressure up to 37 K.[24–26] Further interestingly, $FeTe_{1-x}Se_x$ is also a candidate system of topological superconductor in which a topologically nontrivial band inversion takes places near the Fermi level (E_F) around the Z point,[19] when the superconductivity maintains.

The superconducting transition temperature is greatly enhanced on monolayer $FeTe_{1-x}Se_x$/STO films. Previous low-temperature scanning tunneling microscopy (STM) and scanning tunneling spectroscopy (STS) studies [27] show the significantly enhanced superconducting gap up to 16.5 meV in a wide composition range ($0.1 \le x \le 0.6$) of 1UC $FeTe_{1-x}Se_x$/STO films, with T_c up to above 40 K. Meanwhile, the double and thicker $FeTe_{1-x}Se_x$ films do not show any sign of superconductivity down to 5.7 K. Recently, the angle-resolved photoemission spectroscopy (ARPES) results indicate that the $FeTe_{1-x}Se_x$ monolayer films with low Se concentration are high-temperature connate topological superconductors in which band topology and superconductivity are integrated intrinsically.[28] Thus growing high-quality $FeTe_{1-x}Se_x$/STO monolayer films is crucial for the study of the high-temperature topological superconductors.

In this Letter, we report the detailed growth process and discuss the possible ways to improve the quality of $FeTe_{1-x}Se_x$/STO(001) monolayer films at various substitution levels ($x = 0$, 0.27, 0.33, 0.55, 0.76 and 1). We find that for the growth of FeSe monolayer films, the best treatment temperature of the STO substrate is at around 950℃, the growth temperature at 310℃ and post growth annealing temperature at 380℃. For the $FeTe_{1-x}Se_x$ ($x < 1$), the STO treatment temperature is also around 950℃, while the growth temperature and annealing temperatures both decrease to 260℃. We also study the detailed band structure of $FeTe_{1-x}Se_x$/STO monolayer films by ARPES measurements. We observe clear electron bands around M point in $FeTe_{1-x}Se_x$/STO monolayer films for $x \ge 0.27$, and the superconducting gap feature with transition temperature $T_c \approx 55$ K.

Monolayer films of $FeTe_{1-x}Se_x$ were epitaxially grown on 0.7 wt% Nb-doped STO(001) substrates by the similar process as FeSe/STO(001) described in our previous work.[29] High-purity Fe(99.98%), Te(99.99%) and Se(99.999%) sources were co-

*Supported by the Ministry of Science and Technology of China under Grant Nos 2015CB921000, 2016YFA0401000, 2015CB921301 and 2016YFA0300300, and the National Natural Science Foundation of China under Grant Nos 11274381, 11574371, 11274362, 1190020, 11334012 and 11674371.
**Corresponding author. Email: yjsun@iphy.ac.cn; scw@ruc.edu.cn

evaporated from the Knudsen cells. $FeTe_{1-x}Se_x$ monolayer films were obtained with various Se concentrations. Different Se concentrations are tuned by the flux ratios between Se and Te, which were monitored by quartz crystal balance. The Se concentrations of the films were estimated based on Vegard's law[30,31] and theoretical calculations[9] (shown in the supplemental material).

After growth, the $FeTe_{1-x}Se_x$ monolayer films were annealed to improve crystallinity. The quality of films was identified *in situ* by the reflection high-energy electron diffraction (RHEED), STM and ARPES. The base pressure was 3×10^{-10} Torr in the molecular beam epitaxy (MBE)/STM chamber and better than 3×10^{-11} Torr in the ARPES chamber. ARPES measurements were performed in the same combined system using an R4000 analyzer with a helium discharge lamp. The energy resolution was set to 5 meV for gap measurements and 10 meV for the band structure as well as FS mapping. The angular resolution was set to 0.2°.

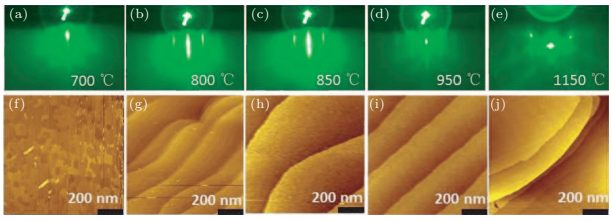

Fig. 1. (Color online) (a)–(e) RHEED patterns of 0.7 wt% Nb-doped STO surface after treated at T_{max} = 700℃, 800℃, 850℃, 950℃ and 1150℃, respectively. (f)–(j) The corresponding STM images of (a)–(e), respectively.

High-quality substrate with atomically flat surface is necessary to grow ultra-flat $FeTe_{1-x}Se_x$/STO monolayer films. Thus we performed precise calibration on substrate treatment prior to deposition and found that the surface smoothness of STO depends on the maximum treatment temperature (T_{max}). At T_{max} = 700℃, a blurred RHEED pattern is observed and no clear STM image is found, indicating a rough surface, as shown in Figs. 1(a) and 1(f), respectively. With the increase of T_{max} to 800℃ and 850℃, the sharpness of RHEED pattern and clarity of the terrace increase, as shown in Figs. 1(b), 1(c), 1(g) and 1(h). The optimal condition reaches T_{max} = 950℃, which yields a sharp RHEED pattern and well aligned terrace, as shown in Figs. 1(d) and 1(i), respectively. With further increasing the treatment temperature, the surface quality starts to degrade. This could be identified at T_{max} = 1150℃, the sharp stripes disappear with the appearance of bright spots, as shown in Fig. 1(e) and STM image shows that layers were bunched, Fig. 1(j), indicating a rough surface. According to Fig. 1, the most appropriate maximum treatment temperature of the STO substrate is $T_{max} \approx 950$℃.

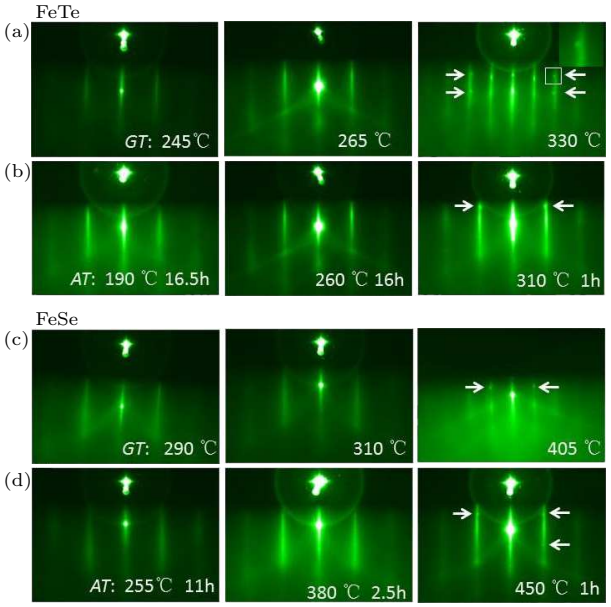

Fig. 2. (Color online) The RHEED patterns of (a) the FeTe films deposited on the STO at GT = 245℃, 265℃ and 330℃, respectively. On the right panel, the upper right corner image is the zoomed view of the white box. (b) FeTe films annealed at AT = 190℃ for 16.5 h, 260℃ for 16 h and 310℃ for 1 h, respectively. (c) FeSe films deposited on the STO at GT = 290℃, 310℃ and 405℃, respectively. (d) FeSe films annealed at AT = 255℃ for 11 h, 380℃ for 2.5 h and 450℃ for 1 h, respectively. The bright dots pointed by the arrows are marks of Fe islands due to Se loss. The straight lines between the bright dots are corresponding FeSe (FeTe) films.

Table 1. The growth process of monolayer $FeTe_{1-x}Se_x$ (x = 0, 0.27, 0.33, 0.55, 0.76 and 1). The STO (Nb: 0.7%) treatment, film deposition, film annealing and superconducting gap are listed. $FeTe_{1-x}Se_x$ ($x \geq 0.27$) are superconductors with gaps feature.

Sample Index	STO treatment	Film deposition	Film annealing	SC gap
#1 FeTe	950℃ for 1.5h	STO at 265℃, Fe at 1225℃, Te at 210℃	265℃ for 5h	N/A
#2 $FeTe_{0.73}Se_{0.27}$	900℃ for 0.5h	STO at 260℃, Fe at 1232℃, Te at 232℃, Se at 68℃	230–260℃ for 14.5h	yes
#3 $FeTe_{0.67}Se_{0.33}$	950℃ for 1.5 h	STO at 261℃, Fe at 1230℃, Te at 230℃, Se at 69℃	250℃ for 12 h	yes
#4 $FeTe_{0.45}Se_{0.55}$	900℃ for 0.5 h	STO at 253℃, Fe at 1232℃, Te at 232℃, Se at 74℃	220–250℃ for 12.5 h	yes
#5 $FeTe_{0.24}Se_{0.76}$	900℃ for 0.5 h	STO at 260℃, Fe at 1230℃, Te at 225℃ Se at 80℃	250℃ for 6 h	yes
#6 FeSe	950℃ for 1.5 h	STO at 310℃, Fe at 1220℃, Se at 86℃	380℃ for 2.5 h	yes

We further investigate the growth and annealing conditions of the FeTe and FeSe films. FeTe films deposited on STO substrates at different growth temperatures (GT) are shown in Fig. 2(a). With increasing GT from T = 245℃ to 265℃, stripes in RHEED image become brighter and sharper. With higher growth temperature, segregation of Fe islands due to the loss of Se atoms will happen,[32,33] as demonstrated by the RHEED of FeTe on STO(110), with GT = 330℃, as shown in the right panel of Fig. 2(a). The growth con-

trol of the FeSe films is compared in Fig. 2(c). The low growth temperature (GT = 290℃, GT = 310℃) and high temperature (GT = 405℃) are compared and the optimal growth condition are reached at GT = 310℃.

After growth, the FeTe films are annealed at annealing temperature (AT) 260℃ for 16 h (Fig. 2(b)) and FeSe at AT = 380℃ for 2.5 h (Fig. 2(d)) to increase the crystallinity. Lower annealing temperature (e.g., AT = 190℃ for FeTe in Fig. 2(b) and AT = 255℃ for FeSe in Fig. 2(d)) will lead to weak stripes indicating low crystallinity. Higher annealing temperature (e.g., AT = 310℃ for FeTe in Fig. 2(b) and AT = 450℃ for FeSe in Fig. 2(d)) will introduce Fe islands. According to these observations, we obtain the optimal growth and annealing temperature of FeTe and FeSe films. Both the optimal GT and AT of the FeTe films are lower than those of FeSe films. These results can be further applied to the growth of $FeTe_{1-x}Se_x$ films.

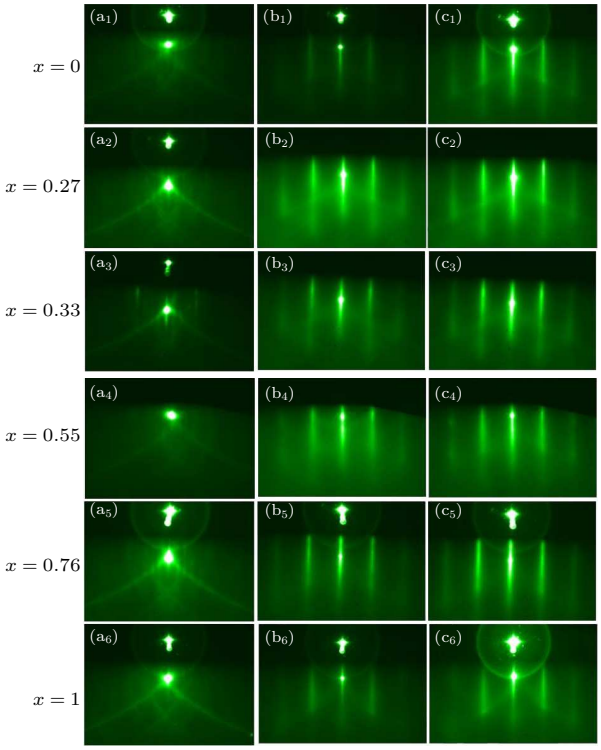

Fig. 3. (Color online) RHEED images of $FeTe_{1-x}Se_x$ monolayer with x = 0, 0.27, 0.33, 0.55, 0.76 and 1, after substrate treatment (a_1)–(a_6), film deposition (b_1)–(b_6) and film annealing (c_1)–(c_6).

Table 1 lists the detailed growth process of 1UC $FeTe_{1-x}Se_x$/STO with x = 0, 0.27, 0.33, 0.55, 0.76, 1 labeled by #1–#6, respectively. The growth process has three stages: STO treatment, film deposition and film annealing. At the first stage, STO substrates with atomically flat surfaces are heated at maximum temperature T_{max} = 900–950℃ for 0.5–1.5 h in accordance with Fig. 1. At the second stage, during deposition, Fe source stays at 1225℃ (±10℃). To tune the Te/Se flux ratio, the temperature of Te (210–230℃) and Se (60–90℃) sources varied according to the measurement of quartz crystal balance. The substrate temperature is GT = 310℃ during depositing FeSe monolayers, and the GT decreases to 260℃ (±10℃) with the decrease of Se concentration, in agreement with Fig. 2. After the growth, the film is annealed at AT=380℃ for FeSe, and AT decreases to 260℃ (±10℃) with the decrease of Se concentration, in agreement with Fig. 2.

Through the growth process, the RHEED with −15 kV and −26 μA was used to monitor the quality of films in real time. The RHEED patterns of STO substrates after treatment for samples #1–#6 are shown in Figs. 3(a_1)–3(a_6), $FeTe_{1-x}Se_x$ films after deposition shown in Figs. 3(b_1)–3(b_6) and after post growth annealing shown in Figs. 3(c_1)–3(c_6), with the parameters described in Table 1. Under these growth conditions, we can observe sharp stripes of RHEED pattern after growth and annealing, which indicate atomically flat surfaces with excellent crystallinity. No extra spots as pointed arrows in Fig. 2 are observed, suggesting no significant Fe island forming in the films.

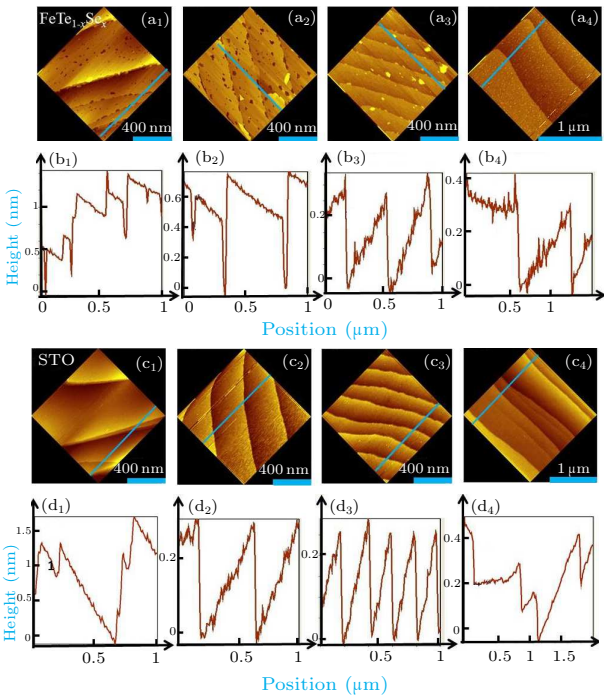

Fig. 4. (Color online) (a) The topographies of $FeTe_{1-x}Se_x$ (x = 0, 0.27, 0.55 and 1) monolayer films. (b) The corresponding line profile along the cuts in images (a). (c) The topographies of the corresponding substrates of $FeTe_{1-x}Se_x$ (x = 0, 0.27, 0.55 and 1). (d) The corresponding line profile along the cuts in images (c). Subscripts 1–4 mark x = 0, 0.27, 0.55, 1, respectively.

The STM images of 1UC $FeTe_{1-x}Se_x$/STO with x = 0, 0.27, 0.55 and 1, and their corresponding of STO substrates are shown in Fig. 4. Figures 4(a_1)–4(a_4) illustrate the topographies of 1UC $FeTe_{1-x}Se_x$ films with various Se concentrations, and the topographies of STO substrates are also shown in Figs. 4(c_1)–4(c_4), respectively. The height profiles are shown in Figs. 4(b_1)–4(b_4) and 4(d_1)–4(d_4) accordingly. From

the STM images and their corresponding height profile of the films, atomically flat surface with size up to few hundred nm could be obtained, with terrace height about few angstrom, consistent with the lattice constant of a FeSe/Te monolayer films. We also noticed few bright spots and black dots on $FeTe_{1-x}Se_x$ films, as shown in Figs. 4(a_1)–4(a_3). The bright spots, mainly seen in Figs. 4(a_2) and 4(a_3), are multilayer $FeTe_{1-x}Se_x$. However, the black dots shown in Figs. 4(a_1) and 4(a_2) are material loss, which can also be identified by the sharp narrow dip in Figs. 4(b_1) and 4(b_2). These multilayer formations and deficiencies are common phenomena in the layer-by-layer growth mode.

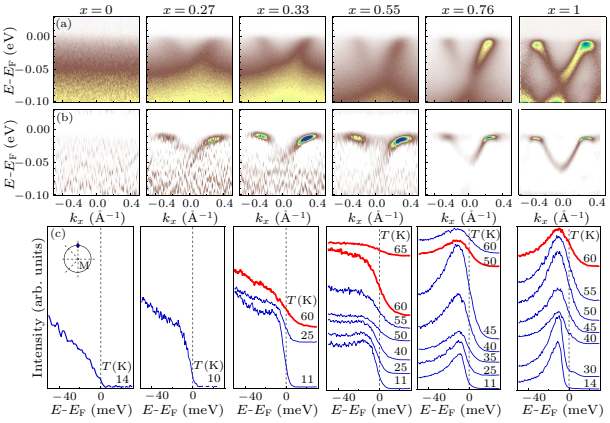

Fig. 5. (Color online) (a) Evolution of ARPES intensity plots around M at 12 K (±2 K), recorded with unpolarized He I photons (21.212 eV), with $x = 0$, 0.27, 0.33, 0.55, 0.76 and 1. (b) Second derivatives intensity plots of (a). (c) Temperature evolution of the EDCs at the k_F point of the electron FS around M for each sample. The red curves correspond nearly to the gap closing temperature.

We performed ARPES studies on a series of $FeTe_{1-x}Se_x$/STO monolayer films. Figure 5(a) shows the band structures around $M(\pi, 0)$ at $T = 12$ K (±2 K) with Se substitution $x = 0$, 0.27, 0.33, 0.55, 0.76, 1, respectively. Figure 5(b) is the corresponding second derivatives of Fig. 5(a). We can see obvious electron bands below E_F at $M(\pi, 0)$ in $FeTe_{1-x}Se_x$/STO monolayer films. With the increase of Se concentration, the band intensity increases and the down-shifts of band bottom are observed. The extracted band mass decreases with the increase of Se substitution, but with negligible change of k_F,[28] suggesting the iso-valence substitution of Te by the Se atom. Figure 5(c) shows the energy distribution curves (EDCs) at k_F of $FeTe_{1-x}Se_x$/STO monolayer films with different Se concentrations. From these EDCs, at the low temperature, $FeTe_{1-x}Se_x$ ($x \geq 0.27$) monolayer film shows similar superconducting gap feature and closing temperature $T_c \approx 50$–60 K defining by the disappearance of superconducting coherence peak[34] (symmetrized EDCs shown in Fig. 5(s1) in the supplemental material). Among all the Se concentrations, the FeSe/STO ($x = 1$) monolayer film has the best defined superconducting quasi-particle peak. The EDC coherent peak degrades with the decrease of Se concentration, which may be due to enhanced electron correlations[8,35] or antiferromagnetic fluctuations.[36]

In summary, we have studied the MBE growth of high-quality $FeTe_{1-x}Se_x$ monolayer films on STO (001) substrates. We illustrate the influence of substrate treatment, growth and annealing temperature on the quality of the films. We obtain the optimal conditions for substrate treatment temperature and FeTe, FeSe films growth and annealing temperatures. With these conditions, we successfully grow a series of $FeTe_{1-x}Se_x$ monolayer films with various Se concentrations. Both RHEED and STM topographies results suggest high quality of the films. From ARPES measurements, the electron bands near $M(\pi, 0)$ and the observation of superconducting gap feature also suggesting the high quality of the $FeTe_{1-x}Se_x$ monolayer films. This research is instructive for further improvements in the crystallinity and surface roughness of $FeTe_{1-x}Se_x$ monolayer films with possible high-temperature topological superconductivity occurring at a low Se concentration.

References

[1] Hsu F C, Luo J Y, Yeh K W, Chen T K, Huang T W, Wu P M, Lee Y C, Huang Y L, Chu Y Y, Yan D C and Wu M K 2008 *Proc. Natl. Acad. Sci. USA* **105** 14262

[2] Yeh K W, Huang T W, Huang Y L, Chen T K, Hsu F C, Wu P M, Lee Y C, Chu Y Y, Chen C L, Luo J Y, Yan D C and Wu M K 2008 *Europhys. Lett.* **84** 37002

[3] Fang M H, Pham H M, Qian B, Liu T J, Vehstedt E K, Liu Y, Spinu L and Mao Z Q 2008 *Phys. Rev.* B **78** 224503

[4] Sales B C, Sefat A S, McGuire M A, Jin R Y, Mandrus D and Mozharivskyj Y 2009 *Phys. Rev.* B **79** 094521

[5] Kamihara Y, Watanabe T, Hirano M and Hosono H 2008 *J. Am. Chem. Soc.* **130** 3296

[6] Bao W, Qiu Y, Huang Q, Green M A, Zajdel P, Fitzsimmons M R, Zhernenkov M, Chang S, Fang M H, Qian B, Vehstedt E K, Yang J H, Pham H M, Spinu L and Mao Z Q 2009 *Phys. Rev. Lett.* **102** 247001

[7] Li S L, de la Cruz C, Huang Q, Chen Y, Lynn J W, Hu J P, Huang Y L, Hsu F C, Yeh K W, Wu M K and Dai P C 2009 *Phys. Rev.* B **79** 054503

[8] Ambolode L C C, Okazaki K, Horio M, Suzuki H, Liu L, Ideta S, Yoshida T, Mikami T, Kakeshita T, Uchida S, Ono K, Kumigashira H, Hashimoto M, Lu D H, Shen Z X and Fujimori A 2015 *Phys. Rev.* B **92** 035104

[9] Wu X X, Qin S S, Liang Y, Fan H and Hu J P 2016 *Phys. Rev.* B **93** 115129

[10] Mizuguchi Y, Tomioka F, Tsuda S, Yamaguchi T and Takano Y 2009 *J. Phys. Soc. Jpn.* **78** 074712

[11] Ding Q P, Mohan S, Tsuchiya Y, Taen T, Nakajima Y and Tamegai T 2011 *Supercond. Sci. Technol.* **24** 075025

[12] Wu M K, Wang M J and Yeh K W 2013 *Sci. Technol. Adv. Mater.* **14** 014402

[13] Chen G F, Chen Z G, Dong J, Hu W Z, Li G, Zhang X D, Zheng P, Luo J L and Wang N L 2009 *Phys. Rev.* B **79** 140509

[14] Liu T J, Hu J, Qian B, Fobes D, Mao Z Q, Bao W, Reehuis M, Kimber S A J, Prokeš K, Matas S, Argyriou D N, Hiess A, Rotaru A, Pham H, Spinu L, Qiu Y, Thampy V, Savici A T, Rodriguez J A and Broholm C 2010 *Nat. Mater.* **9** 718

[15] Gawryluk D J, Fink-Finowicki J, Wiśniewski A, Puźniak R, Domukhovski V, Diduszko R, Kozłowski M and Berkowski M 2011 *Supercond. Sci. Technol.* **24** 065011

[16] Huang C L, Chou C C, Tseng K F, Huang Y L, Hsu F C, Yeh K W, Wu M K and Yang H D 2009 *J. Phys. Soc. Jpn.* **78** 084710
[17] Kantarcı Güler N, Ekicibil A, Özçelik B, Onar K, Yakıncı M E, Okazaki H, Takeya H and Takano Y 2014 *J. Supercond. Novel Magn.* **27** 2691
[18] Nakayama K, Sato T, Richard P, Kawahara T, Sekiba Y, Qian T, Chen G F, Luo J L, Wang N L, Ding H and Takahashi T 2010 *Phys. Rev. Lett.* **105** 197001
[19] Wang Z J, Zhang P, Xu G, Zeng L K, Miao H, Xu X Y, Qian T, Weng H M, Richard P, Fedorov A V, Ding H, Dai X and Fang Z 2015 *Phys. Rev.* B **92** 115119
[20] Miao H, Richard P, Tanaka Y, Nakayama K, Qian T, Umezawa K, Sato T, Xu Y M, Shi Y B, Xu N, Wang X P, Zhang P, Yang H B, Xu Z J, Wen J S, Gu G D, Dai X, Hu J P, Takahashi T and Ding H 2012 *Phys. Rev.* B **85** 094506
[21] Lubashevsky Y, Lahoud E, Chashka K, Podolsky D and Kanigel A 2012 *Nat. Phys.* **8** 309
[22] Zhang P, Richard P, Xu N, Xu Y M, Ma J, Qian T, Fedorov A V, Denlinger J D, Gu G D and Ding H 2014 *Appl. Phys. Lett.* **105** 172601
[23] Hanaguri T, Niitaka S, Kuroki K and Takagi H 2010 *Science* **328** 474
[24] Mizuguchi Y, Tomioka F, Tsuda S, Yamaguchi T and Takano Y 2008 *Appl. Phys. Lett.* **93** 152505
[25] Medvedev S, McQueen T M, Troyan I A, Palasyuk T, Eremets M I, Cava R J, Naghavi S, Casper F, Ksenofontov V, Wortmann G and Felser C 2009 *Nat. Mater.* **8** 630
[26] Margadonna S, Takabayashi Y, Ohishi Y, Mizuguchi Y, Takano Y, Kagayama T, Nakagawa T, Takata M and Prassides K 2009 *Phys. Rev.* B **80** 064506
[27] Li F S, Ding H, Tang C J, Peng J P, Zhang Q H, Zhang W H, Zhou G Y, Zhang D, Song C L, He K, Ji S H, Chen X, Gu L, Wang L L, Ma X C and Xue Q K 2015 *Phys. Rev.* B **91** 220503
[28] Shi X, Han Z Q, Richard P, Wu X X, Peng X L, Qian T, Wang S C, Hu J P, Sun Y J and Ding H 2017 *Sci. Bull.* **62** 503
[29] Shi X, Han Z Q, Peng X L, Richard P, Qian T, Wu X X, Qiu M W, Wang S C, Hu J P, Sun Y J and Ding H 2017 *Nat. Commun.* **8** 14988
[30] Vegard L 1921 *Z. Für Phys.* **5** 17
[31] Denton A R and Ashcroft N W 1991 *Phys. Rev.* A **43** 3161
[32] Stroscio J A, Pierce D T and Dragoset R A 1993 *Phys. Rev. Lett.* **70** 3615
[33] Korobtsov V V, Balashev V V and Pisarenko T A 2007 *E-J. Surf. Sci. Nanotech.* **5** 45
[34] Umezawa K, Li Y, Miao H, Nakayama K, Liu Z H, Richard P, Sato T, He J B, Wang D M, Chen G F, Ding H, Takahashi T and Wang S C 2012 *Phys. Rev. Lett.* **108** 037002
[35] Ieki E, Nakayama K, Miyata Y, Sato T, Miao H, Xu N, Wang X P, Zhang P, Qian T, Richard P, Xu Z J, Wen J S, Gu G D, Luo H Q, Wen H H, Ding H and Takahashi T 2014 *Phys. Rev.* B **89** 140506
[36] Manna S, Kamlapure A, Cornils L, Hänke T, Hedegaard E M J, Bremholm M, Iversen B B, Hofmann P, Wiebe J and Wiesendanger R 2017 *Nat. Commun.* **8** 14074

Supplemental Material for

High-quality $FeTe_{1-x}Se_x$ monolayer films on $SrTiO_3$(001) substrates grown by molecular beam epitaxy

Zhi-Qing Han(韩智卿)[1], Xun Shi(施训)[2], Xi-Liang Peng(彭锡亮)[2], Yu-Jie Sun(孙煜杰)[2*] and Shan-Cai Wang(王善才)[1*]

[1] Department of Physics, Beijing Key Laboratory of Opto-Electronic Functional Materials and Micro-nano Devices, Renmin University of China, Beijing 100872, People's Republic of China
[2] Beijing National Laboratory for Condensed Matter Physics, and Institute of Physics, Chinese Academy of Sciences, Beijing 100190, People's Republic of China

[*]Email: yjsun@iphy.ac.cn, scw@ruc.edu.cn

Definition of Se concentrations:

We have grown samples with different Se concentrations by tuning the flux ratios between Se and Te, which were monitored by quartz crystal balance.

According to Vegard's law [1] [2] and theoretical calculations [3] on $FeTe_{1-x}Se_x$ thin films, band positions (electron band bottom or hole band top) at Γ should vary linearly with Se concentrations. Thus, we measured the band positions at Γ of different flux ratios. To make the band positions linearly with the Se concentrations, we multiplied all the different flux ratios by a same factor, and the results (shown in fig.S1) correspond to the Se concentrations of our manuscript.

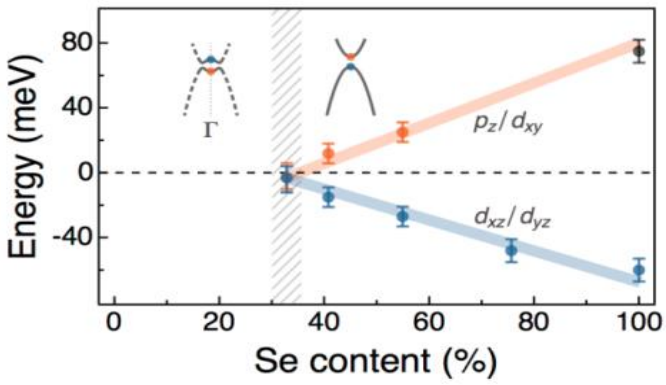

Fig.S1. Evolution of the band positions at Γ [4]. The electron-like band position of FeSe/STO is adapted from Ref. [5].

Figure 5 S1:

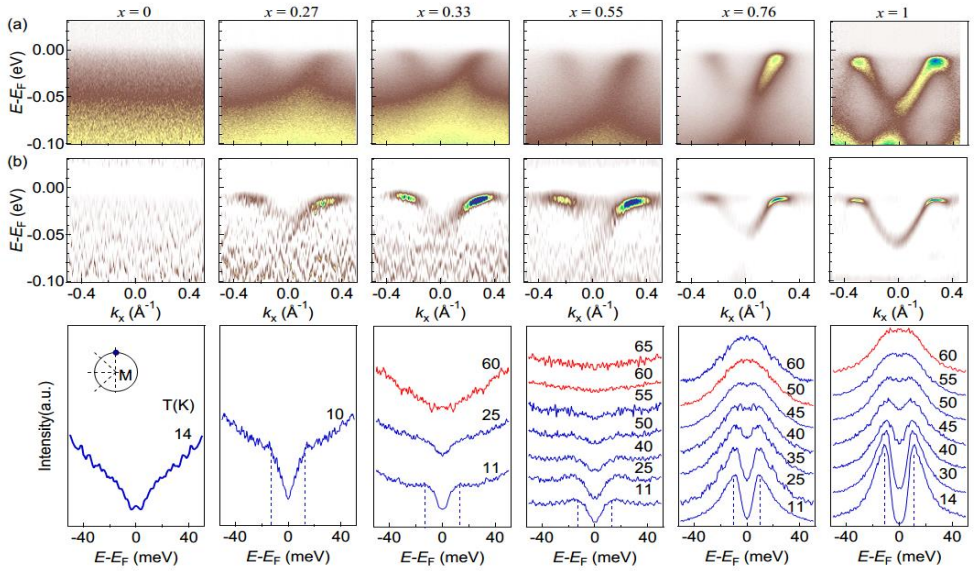

(a) Evolution of ARPES intensity plots around M at 12 K(±2 K), recorded with unpolarized He Iα photons (21.212 eV), with x = 0, 0.27, 0.33, 0.55, 0.76, 1. (b) second derivatives intensity plots of (a). (c) Temperature evolution of the symmetrized EDCs at the k_F point of the electron FS around M for each sample. The red curves correspond nearly to the gap closing temperature.

References:

1. Vegard, L. Die Konstitution der Mischkristalle und die Raumfüllung der Atome. Zeitschrift für Physik. 5(1): 17–26(1921).
2. A. R. Denton and N. W. Ashcroft. Vegard's law. Phys. Rev. A 43(6): 3161–3164(1991).
3. X. Wu, S. Qin, Y. Liang, H. Fan, J. Hu. Topological characters in $Fe(Te_{1-x}Se_x)$ thin films. Phys. Rev. B93, 115129(2016).
4. X. Shi, Z.-Q. Han, P. Richard, X.-X. Wu, X.-L. Peng, T. Qian, S.-C. Wang, J.-P. Hu, Y.-J. Sun, and H. Ding, Science Bulletin 62, 503 (2017).
5. Huang D, Song CL, Webb TA, et al. Revealing the empty-state electronic structure of single-unit-cell FeSe/SrTiO3. Phys Rev Lett 115:017002 (2015).